Journal of Neurochemistry

JOURNAL OF NEUROCHEMISTRY | 2013 | 126 | 360–371 doi: 10.1111/jnc.12306

ORIGINAL ARTICLE

Novel contribution of cell surface and intracellular M1-muscarinic acetylcholine receptors to synaptic plasticity in hippocampus

Abu Syed Md Anisuzzaman,*,[1] Junsuke Uwada,*,†,[1] Takayoshi Masuoka,‡,[1] Hatsumi Yoshiki,* Matomo Nishio,‡ Yuji Ikegaya,§ Naoya Takahashi,§ Norio Matsuki,§ Yasuhisa Fujibayashi,¶ Yoshiharu Yonekura,¶ Toshihiko Momiyama** and Ikunobu Muramatsu*,†,††

*Division of Pharmacology, Department of Biochemistry and Bioinformative Sciences, School of Medicine, University of Fukui, Eiheiji, Japan

†Organization for Life Science Advancement Programs, University of Fukui, Eiheiji, Japan

‡Department of Pharmacology, School of Medicine, Kanazawa Medical University, Uchinada, Japan

§Laboratory of Chemical Pharmacology, Graduate School of Pharmaceutical Sciences, The University of Tokyo, Hongo Bunkyo-ku, Japan

¶Biomedical Imaging Research Center, University of Fukui, Eiheiji, Japan

**Department of Pharmacology, Jikei University School of Medicine, Minato-ku, Japan

††Child Development Research Center, Graduate School of Medicine, University of Fukui, Eiheiji, Japan

Abstract

Muscarinic acetylcholine receptors (mAChRs) are well known to transmit extracellular cholinergic signals into the cytoplasm from their position on the cell surface. However, we show here that M1-mAChRs are also highly expressed on intracellular membranes in neurons of the telencephalon and activate signaling cascades distinct from those of cell surface receptors, contributing uniquely to synaptic plasticity. Radioligand-binding experiments with cell-permeable and -impermeable ligands and immunohistochemical observations revealed intracellular and surface distributions of M1-mAChRs in the hippocampus and cortex of rats, mice, and humans, in contrast to the selective occurrence on the cell surface in other tissues. All intracellular muscarinic-binding sites were abolished in M1-mAChR-gene-knockout mice. Activation of cell surface M1-mAChRs in rat hippocampal neurons evoked phosphatidylinositol hydrolysis and network oscillations at theta rhythm, and transiently enhanced long-term potentiation. On the other hand, activation of intracellular M1-mAChRs phosphorylated extracellular-regulated kinase 1/2 and gradually enhanced long-term potentiation. Our data thus demonstrate that M1-mAChRs function at both surface and intracellular sites in telencephalon neurons including the hippocampus, suggesting a new mode of cholinergic transmission in the central nervous system.

Keywords: cell surface and intracellular GPCR, ERK1/2, LTP, M1-muscarinic receptor, synaptic plasticity.

J. Neurochem. (2013) **126**, 360–371.

Among the five muscarinic acetylcholine receptor (mAChR) subtypes, M1-mAChRs predominantly exist in the CNS and are involved in cognitive enhancement (Wess 2004;

Received March 6, 2013; revised manuscript received April 30, 2013; accepted May 14, 2013.

Address correspondence and reprint requests to Ikunobu Muramatsu, Division of Pharmacology, Department of Biochemistry and Bioinformative Sciences, School of Medicine, University of Fukui, Eiheiji, Fukui 910-1193, Japan. E-mail: muramatu@u-fukui.ac.jp

[1]These authors contributed equally to this study.

Abbreviations used: ACh, acetylcholine; ACSF, artificial cerebrospinal fluid; CCh, carbachol; EGR-1, early growth response-1; ERK1/2, extracellular regulated kinase 1/2; fEPSP, field excitatory post-synaptic potential; GPCR, G-protein coupled receptor; HFS, high-frequency stimulation; LTP, long-term potentiation; mAChR, muscarinic acetylcholine receptor; MAPK, mitogen-activated protein kinase; MT-7, muscarinic toxin-7; NMDAR, *N*-methyl-D-aspartate receptor; NMS, *N*-methyl-scopolamine; PI, phosphatidylinositol; PLC, phospholipase C; QNB, qunuclidinyl benzilate; TTX, tetrodotoxin.

Yamasaki *et al.* 2010). M1-mAChR-knockout mice show severe deficits in working memory and memory consolidation, and impaired long-term potentiation (LTP) in the hippocampus (Anagnostaras *et al.* 2003; Shinoe *et al.* 2005; Wess *et al.* 2007), a primary experimental model for the synaptic basis of learning and memory (Bliss and Collingridge 1993; Seol *et al.* 2007). Furthermore, M1-specific agonists facilitate the induction of LTP and improve cognitive function in several animal models of amnesia (Caccamo *et al.* 2006; Langmead *et al.* 2008; Ma *et al.* 2009). Biochemically, M1-mAChRs associated with $G_{q/11}$ protein are well known to cause phosphatidyl inositol (PI) hydrolysis leading to Ca^{2+} up-regulation and activation of the MAPK pathway (van Koppen and Kaiser 2003; Wess 2004). However, the mechanisms by which M1-mAChRs and the associated signaling cascades contribute to physiological functions in the CNS remain unclear.

Most G-protein-coupled receptors (GPCRs), including mAChRs, are generally believed to signal from locations on the cell surface, but evidence is accumulating that several GPCRs are also located in, and may signal from, intracellular sites, such as endosomes/clathrin-coated pits, endoplasmic reticulum (ER), Golgi apparatus, and nuclear membranes (Boivin *et al.* 2008; Jong *et al.* 2009; den Boon *et al.* 2012). Using N1E-115 neuroblastoma cells, we recently demonstrated that M1-mAChRs are expressed not only on the plasma membrane, but also on intracellular membranes, and that M1-mAChRs at both sites are independently activated by muscarinic agonists (ACh and carbachol) (Uwada *et al.* 2011). However, whether such geographically distinct M1-mAChRs are present and physiologically function in the mammalian brain remains unclear.

Here, we report cell surface and intracellular distributions of M1-mAChRs in the higher brain regions of rodents and humans and their unique involvement in cholinergic functions of CNS.

Methods

Animals and tissue isolation

Animal handling and all experimental procedures were performed according to the Guidelines for Animal Experiments, University of Fukui, Kanazawa Medical University, The University of Tokyo and Jikei University School of Medicine. These procedures were approved by the Animal Care and Use committees of the four universities mentioned above. Rats and mice were housed in a temperature (23°C)- and humidity (45%)-controlled environment on a 12 h light/dark cycle (lights on at 8 : 00 am). Food and water were available *ad libitum*.

Male Wistar rats (Charles River Japan, Yokohama, Japan) were used, with age ranges from 8 to 10 weeks for binding and 2.5–6 weeks for electrophysiological experiments. M1-mAChR-knockout mice (on a mixed 129/SvJ and C57BL/6 genetic background) were obtained from the Center for Animal Resources and Development, Kumamoto University (Kumamoto, Japan). Generation of homozygous M1-mAChR-knockout mice has been described previously (Shinoe *et al.* 2005). Littermates of male wild-type and M1-mAChR-knockout mice at 5–6 weeks were used for binding experiments. Rats and mice were anesthetized with isoflurane or halothane, and the brain, urinary bladder and stomach were rapidly excised and placed in a modified Krebs-Henseleit solution that had been aerated with a mixture of 95% O_2 and 5% CO_2 and maintained at 0–4°C (pH 7.4) beforehand. Composition of the modified Krebs-Henseleit solution was 112 mM NaCl, 5.9 mM KCl, 1.2 mM $MgCl_2$, 2 mM $CaCl_2$, 1.2 mM $NaHPO_4$, 25 mM $NaHCO_3$, and 11.5 mM glucose.

Human tissues

Human cerebral cortex and urinary bladder tissues were obtained during the course of post-mortem or prescribed surgery, respectively, after obtaining University of Fukui Ethics Committee approval and consent from the patients. Donors were 56–78 years old for cortex (two males and one female) and 53–81 years old for urinary bladder (three males and one female). None of the donors had undergone radiotherapy. All isolated specimens were macroscopically normal, without any signs of tumor or inflammation. The cerebral cortex (frontal lobe) and the urinary bladder (detrusor muscle) were carefully dissected out under a dissection microscope and applied to segment binding assay. The sizes of human tissue segments were approximately 3 × 3 × 1 mm for cerebral cortex and 4 × 3 × 2 mm for detrusor muscle.

Primary neuronal culture

Fetal rats and mice (18 days gestation) were anesthetized with halothane and decapitated. Hippocampus and cerebral cortex were dissected from the fetus and trypsinized for 13 min at 37°C. After filtration through nylon mesh, the neurons were cultured in Neurobasal medium with 10% dialyzed horse serum, GlutaMAX (Invitrogen, Carlsbad, CA, USA), B27 and antibiotics (penicillin and streptomycin). After 16–20 h, the culture medium was replaced with serum-free Neurobasal medium supplemented with B27, antibiotics, and 1 μM cytosine arabinoside to prevent proliferation of non-neuronal cells. Half amount of the medium was replaced for new medium on day 7. After 14 day culture, cells were used for each experiment.

Segment and whole-cell binding experiments

Tissue segment binding was performed as described previously (Anisuzzaman *et al.* 2011). Briefly, the tissue segments isolated from rats, mice, and human were incubated with 1-[*N*-methyl-^{3}H] scopolamine ([^{3}H]NMS) or 1-quinuclidinyl-[phenyl-4-^{3}H]-benzilate ([^{3}H]QNB) in a modified Krebs–Henseleit solution. The concentrations of both radioligands were 0.1–5 nM in saturation experiments and 2 nM in competition experiments. Binding incubation was performed at 4°C for 26–28 h in a final volume of 1 mL, then the segments were washed into a plastic tube containing 1.5 mL of ice-cold incubation solution (4°C) by vortex mixing for 1 min. Segments were then solubilized in 0.3 M NaOH solution to estimate the bound radioactivity and protein content. In whole-cell binding experiments, hippocampal and cortical cultured neurons were incubated for 4 h at 4°C in the incubation solution mentioned above, then the cells were washed using the cell harvester. Non-specific binding was determined in the presence of 1 μM atropine. Bound radioactivity was measured using a liquid scintillation counter. Protein concentration in each tissue segment was measured using a protein assay kit (Bio-

Rad Laboratories, Richmond, CA, USA). Experiments were performed in duplicate at each concentration.

Immunohistochemical observation

Primary hippocampal and cortical neurons of rats and mice were grown on poly-L-lysine-coated glass coverslips for 14 days. Immunofluorescence using confocal microscopy was carried out as previously described (Uwada *et al.* 2011). Primary antibodies were anti-M1-mAChR (Frontier Institute, Hokkaido, Japan), anti-GM130 (BD Biosciences, San Jose, CA, USA), anti-Na^+/K^+-ATPase α1 (C464.6), and anti-$G_{q/11}$ protein (E-17) (Santa Cruz Biotechnology Inc., Santa Cruz, CA, USA). Secondary antibodies were Dylight488 conjugated anti-mouse immunoglobulin (Ig)G and Cy3 conjugated anti-rabbit IgG (Jackson ImmunoResearch, West Grove, PA, USA). Coverslips were mounted on slide glasses using glycerol-DABCO. Images were obtained with a confocal microscope (TCS-SP2-AOBS; Leica Microsystems, Wetzlar, Germany).

Western blotting

On day 14 *in vitro*, cultured neurons from rats were treated with 100 μM carbachol for 5 min in the absence or presence of antagonists or inhibitors that had been added 15 min prior to carbachol addition. After carbachol treatment, cells were collected using sodium dodecyl sulfate sample buffer-containing several phosphatase inhibitors, and subjected to sodium dodecyl sulfate polyacrylamide gel electrophoresis followed by transfer to polyvinylidine fluoride membranes (GE Healthcare, Piscataway, NJ, USA). The same sample was probed using anti-phospho- extracellular-regulated kinase (ERK)1/2 and anti-ERK1/2 (Cell Signaling Technology, Beverly, MA, USA) antibodies and the ratio of phospho-ERK1/2 to total ERK was quantified by densitometry.

Measurement of phosphoinositide hydrolysis

Phosphoinositide hydrolysis in the cultured neurons of rats was determined by monitoring the accumulation of inositol monophosphates in [^{3}H]inositol-preloaded preparations, as reported previously (Uwada *et al.* 2011). Experiments were performed throughout the presence of 1 μM tetrodotoxin.

Electrophysiological experiments – field recording

Rats (5–6 weeks old) were anesthetized with inhalation of isoflurane and decapitated. The isolated hippocampus was cut by a vibratome (PRO7, Dosaka, Kyoto, Japan) into 400 μm thick slices in an ice-cold cutting solution containing 110 mM choline chloride, 25 mM glucose, 25 mM $NaHCO_3$, 11.5 mM sodium ascorbate, 7 mM $MgCl_2$, 3 mM sodium pyruvate, 2.5 mM KCl, 1.25 mM NaH_2PO_4, and 0.5 mM $CaCl_2$ (bubbled with 95% O_2 and 5% CO_2 to maintain pH 7.4). Slices were then equilibrated with artificial cerebrospinal fluid containing 138.6 mM NaCl, 3.35 mM KCl, 21 mM $NaHCO_3$, 9.9 mM glucose, 0.6 mM NaH_2PO_4, 2.5 mM $CaCl_2$, and 1 mM $MgCl_2$ (bubbled with 95% O_2 and 5% CO_2 to maintain pH 7.4) at 21–26°C for at least 1 h and transferred to the recording chamber mounted on a microscope stage with continuous superfusion of artificial cerebrospinal fluid at 1–2 mL/min at 30°C. To record theta oscillations, local field potentials were recorded from CA3b stratum radiatum with glass microelectrodes filled with 3 M NaCl (1–2 MΩ) using a MultiClamp 700B (Molecular Devices, Union City, CA, USA), because the CA3 region contains an intrinsic oscillatory network that generates intra-hippocampal theta oscillations that propagate to the CA1 region (Fellous and Sejnowski 2000; Buzsaki 2002).

Data were digitized at 10 kHz and low-pass filtered at 200 Hz. Theta-wave power was calculated by measuring the ratio of the power within the theta band (4–12 Hz) to the total power in the power spectrum.

For recording LTP in CA1 synapses, extracellular recordings using a MultiClamp 700A (Molecular Devices) were obtained with glass pipettes (0.5–1 MΩ) filled with 3 M NaCl and placed within the stratum radiatum. Synaptic responses were evoked by stratum radiatum stimulation (0.1 ms, 30–70 μA) more than 200 μm distant to the recording electrodes. Stimulus intensity was normally set at about 30–40% of the intensity that the evoked maximal slope of the field excitatory post-synaptic potential (fEPSP), and stimuli were applied every 10 s for at least 15 min prior to drug application. A standard high-frequency stimulation (HFS, 100 Hz for 1 s) was used to induce LTP and slopes of fEPSPs were monitored for 60 min. In each recording, fEPSP slopes in initial 10 min were normalized as 100%. In preliminary experiments, we confirmed that the HFS-induced LTP was suppressed by an antagonist of *N*-methyl-D-aspartate receptor (NMDAR, 50 μM DL-AP5), suggesting that the LTP evoked here was dependent on the activation of NMDARs (Pawlak *et al.* 2005).

Electrophysiological experiments – whole-cell recording

Rats (18–22 days old) were decapitated under deep halothane anesthesia, and hippocampi were quickly removed (Shimuta *et al.* 2001). Transverse hippocampal slices (300 μm thick) were cut using a microslicer (PRO7; Dosaka, Kyoto, Japan) in ice-cold oxygenated cutting Krebs solution containing 120 mM choline chloride, 2.5 mM KCl, 0.5 mM $CaCl_2$, 7 mM $MgCl_2$, 1.25 mM NaH_2PO_4, 26 mM $NaHCO_3$, 15 mM D-glucose, 1.3 mM ascorbic acid. Slices were then transferred to a holding chamber containing a standard Krebs solution (Momiyama and Fukazawa 2007) bubbled with 95% O_2 and 5% CO_2 at 21–26°C for at least 1 h before recording. For recording, a slice was transferred to the recording chamber, held submerged, and superfused with Krebs solution (bubbled with 95% O_2-5% CO_2) at a rate of 3–4 mL min^{-1}. Pyramidal neurons within the CA1 region were visually identified with a 60 × water immersion objective attached to an upright microscope (BX50WI; Olympus Optics, Tokyo, Japan). Images were detected with a cooled CCD camera (CCD-300T-RC; Nippon Roper, Tokyo, Japan) and displayed on a video monitor (LC-150M1; SHARP, Tokyo, Japan). Pipettes for whole-cell recordings were made from standard-walled borosilicate glass capillaries (outer diameter, 1.5 mm; Clark Electromedical, Reading, UK). Patch pipettes were filled with a K-gluconate-based internal solution (Momiyama and Fukazawa 2007). Whole-cell recordings were made from visually identified pyramidal neurons in the CA1 region with a patch-clamp amplifier (Axopatch 200B; Molecular Device, Foster City, CA, USA), as reported previously (Momiyama and Fukazawa 2007). Synaptic currents were evoked by extracellularly delivered voltage pulses (duration, 0.2–0.4 ms) of suprathreshold intensity via a glass stimulating electrode filled with 1 M NaCl. The stimulating electrode was placed in the stratum radiatum, and Schaffer collateral/commissural fibers were stimulated at 0.1 Hz. All excitatory post-synaptic currents (EPSCs) were evoked at a holding

potential of −60 mV in the presence of D-AP5 (25 μM), strychnine (0.5 μM), and bicuculline (10 μM) to block NMDA-, glycine-, and $GABA_A$ receptor-mediated current components, respectively. Evoked EPSCs were reversibly blocked by bath application of 5 μM CNQX (an AMPA/kainite receptor antagonist), indicating the non-NMDR-mediated response. Experiments were carried out at 21–26°C.

However, it should be noted that the both LTP analyses mentioned above have been carried out under non-physiological conditions, since the glucose concentrations in the standard cutting and perfusing solutions for the brain slice preparation were much higher than physiological levels.

Data analysis

Binding data were analyzed using Prism software (Graph Pad Software, San Diego, CA, USA), as described previously (Uwada *et al.* 2011). All data were expressed as mean ± SEM and were tested using analysis of variance followed by Bonferroni's *post hoc* test when needed. Differences were considered significant for values of $p < 0.05$.

Materials

Compounds were purchased from commercial sources as follows: 1-[^{3}H]NMS (specific activity 3.00 TBq/mmol) and 1-[^{3}H]QNB (specific activity 1.81 TBq/mmol) from Amersham Biosciences (Buckinghamshire, UK), [methyl-^{3}H]-acetylcholine iodide (specific activity 85 Ci/mmol) from American Radiolabeled Chemicals (St. Louis, MO, USA), atropine sulfate and tetrodotoxin from Nacalai Tesque (Kyoto, Japan), carbachol and pirenzepine from Sigma-Aldrich (St. Louis, MO, USA), AFDX-116 from Tocris (Ellisville, MO, USA), PD98059 from Calbiochem (San Diego, CA, USA), darifenacin from Ono Pharmaceutical (Osaka, Japan), muscarinic toxin-3 (MT3) and muscarinic toxin-7 (MT7) from Peptide Institute (Osaka, Japan). YM-254890 was kindly donated by Dr. J. Takasaki (Yamanouchi Pharmaceutical, Ibaraki, Japan).

Results

Surface and intracellular distribution of M1-mAChRs in hippocampus and other tissues

Subcellular distribution of mAChRs can be pharmacologically identified using the different physicochemical properties of ligand probes. Here, we applied two distinct radioligands, hydrophilic [^{3}H]NMS and hydrophobic [^{3}H]QNB, to intact tissue segments or whole cells to detect total (QNB binding) and cell surface (NMS-binding) mAChRs. Fig. 1a, shows mAChR densities estimated from saturation-

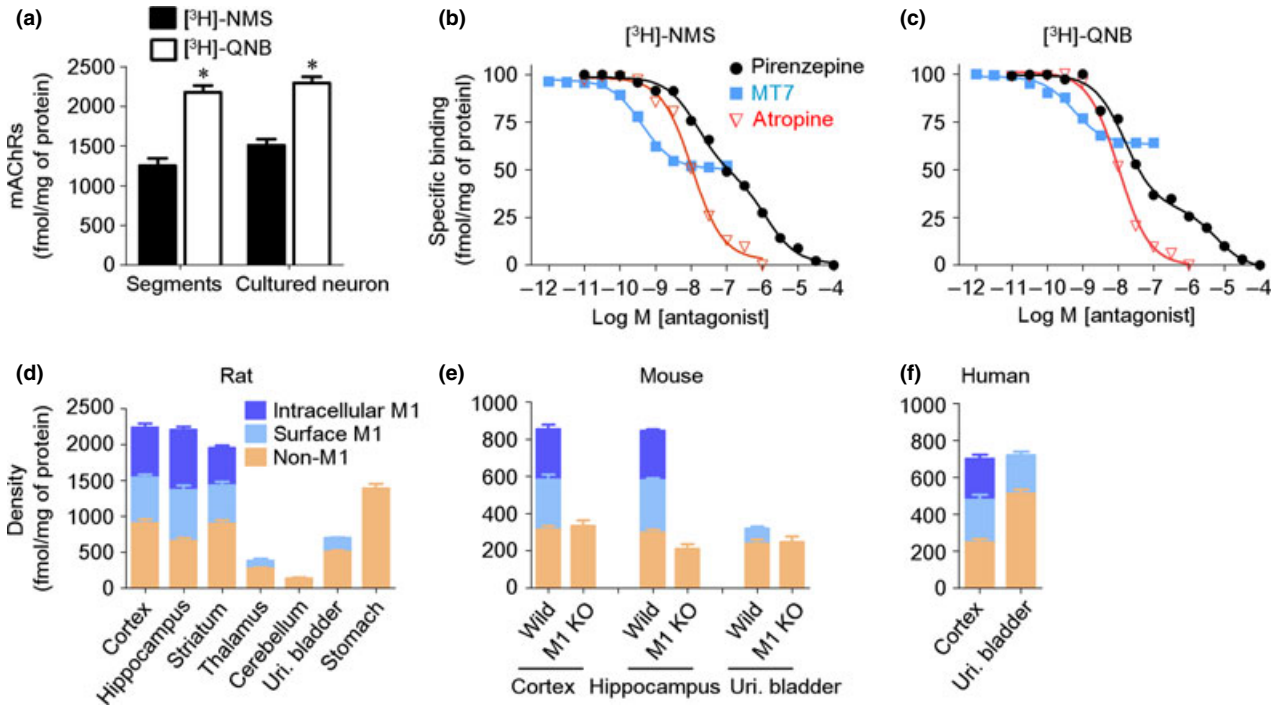

Fig. 1 Surface and intracellular distribution of M1-muscarinic acetylcholine receptors (mAChRs). (a) Densities of mAChRs estimated by hydrophilic [^{3}H] *N*-methyl-scopolamine (NMS) and hydrophobic [^{3}H] qunuclidinyl benzilate (QNB) in rat hippocampal tissue segments ($n = 8$) and primary neurons ($n = 4$). Non-specific binding was defined as the binding in the presence of 1 μM atropine (approximately 9.4% and 22% of total binding of 2000 pM [^{3}H]NMS and [^{3}H]QNB in the segments, and 7% and 11% in the cultured neurons, respectively). *$p < 0.05$ between both radioligand binding sites. (b, c) Competition curves for MT7, pirenzepine and atropine at surface (b) and total (c) mAChRs in rat hippocampal segments. These are representatives of four to five experiments. (d–f) Distributions of intracellular M1-mAChRs, surface M1-mAChRs, and non-M1-mAChRs in tissue segments from rats ($n = 5$) (d), wild-type and M1-knockout (M1-KO) mice ($n = 4$) (e) and humans ($n = 3$–4) (f). Uri. Bladder and stomach: detrusor and gastric body muscles were used respectively. Error bars denote SEM.

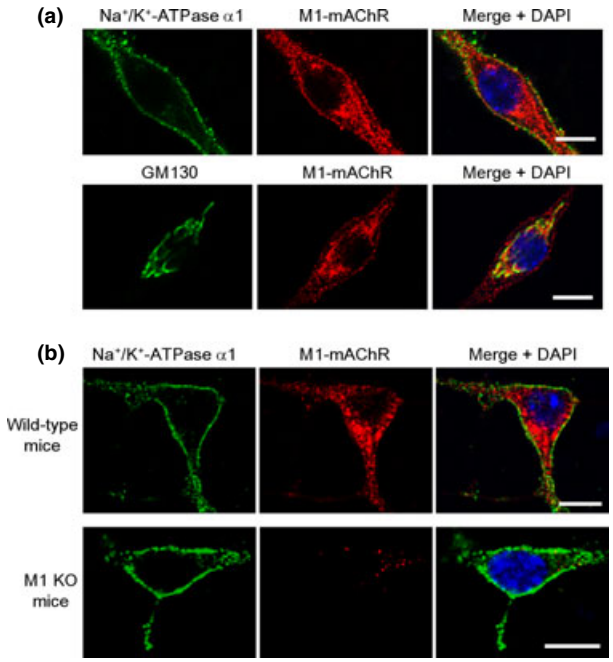

Fig. 2 Subcellular localization of M1-muscarinic acetylcholine receptors (mAChRs) by confocal microscopy. (a, b) Immunostaining of anti-M1-mAChR antibody (red), anti-Na^+/K^+ATPase α1 (plasma membrane marker, green), and anti-GM130 (Golgi marker, green) in primary neurons of rat hippocampus (a), and wild-type and M1-KO mouse cortex (b). Merged images include DAPI staining (nucleus, blue). All images in (a and b) are single confocal sections. Scale bars, 10 μm. The same results were obtained from four experiments.

binding assays with each radioligand in rat hippocampal tissues and primary cultured hippocampal neurons. The density of mAChRs detected by cell-permeable hydrophobic [^{3}H]QNB was approximately 2300 fmol/mg protein in both preparations, significantly higher than the density detected by hydrophilic cell-impermeable [^{3}H]NMS (1400–1500 fmol/mg protein). Binding experiments were conducted under conditions that kept cells intact, and at a low temperature of 4°C; so the higher density of [^{3}H]QNB binding sites compared to [^{3}H]NMS-binding sites implies the presence of additional mAChRs at locations inaccessible to hydrophilic NMS (i.e., the presence of intracellular mAChRs). Competition curves for muscarinic toxin MT7 (cell-impermeable M1 antagonist) and pirenzepine (M1/M4 antagonist) showed that approximately 50% of surface mAChRs ([^{3}H]NMS binding sites) were of M1 subtype (pKi = 9.7 for MT7 and 7.9 for pirenzepine, respectively) (Fig. 1b). Conversely, approximately 70% of all mAChRs ([^{3}H]QNB binding sites) exhibited a high affinity for pirenzepine (pKi = 7.9), and half of these were also sensitive to cell-impermeable MT7 (pKi = 9.3) (Fig. 1c). The same results were obtained in rat cerebral cortex (data not shown). M4-mAChRs were also identified in the competition experiments with muscarinic toxin MT3 (pKi = 8.9), but the proportion of M4 subtype was less than 10% of total mAChRs. M1-mAChRs were thus the most abundant mAChR subtype in the rat hippocampus and cerebral cortex, and half the population of M1-mAChRs was located at intracellular sites and recognized by pirenzepine but not by MT7 under intact tissue conditions (Fig. 1d). The other mAChR subtypes (non-M1 sites) were insensitive to MT7, and were located at the surface membrane only. Therefore, we concluded that total mAChR density and surface/intracellular populations of M1-mAChRs can be estimated from the saturation experiments with cell-permeable hydrophobic [^{3}H]QNB and the competition experiments with cell-impermeable MT7 and cell-permeable pirenzepine.

This pharmacological approach was applied to other tissue segments of rats, showing that the intracellular distribution of M1-mAChRs is unique in hippocampus, cerebral cortex and striatum (Fig. 1d). In rat thalamus and urinary bladder muscle, however, M1-mAChRs were localized at the cell surface only. Surface and intracellular M1-mAChRs were detected in the cerebral cortex and hippocampus of wild-type mice, but were not observed in M1-mAChR-gene-knockout mice (Fig. 1e). Thus, the pharmacologically identified surface and intracellular M1-mAChRs are likely to originate from a single M1-mAChR gene. Surface and intracellular distributions of M1-mAChRs were also identified in human cerebral cortex, but intracellular M1-sites were not detected in human urinary bladder muscle (Fig. 1f). Intracellular distribution of M1-mAChRs was thus considered unique to telencephalon of mammals, including humans.

Immunofluorescence studies also indicated that M1-mAChRs were distributed not only at the cell surface but also at intracellular components corresponding to Golgi apparatus in rat hippocampal neurons (Fig. 2a). Surface and intracellular M1-mAChR immunofluorescence signals were not detected in the cortical neurons obtained from M1-mAChR gene-knockout mice (Fig. 2b). These data are in good agreement with recent immunoelectron microscopic observations, in which a significant number of intracellular M1-mAChRs have been associated with the Golgi and ER compartments in the pyramidal neurons of mouse cerebral cortex and hippocampus (Yamasaki *et al.* 2010).

Signaling cascades activated by surface and intracellular M1-mAChRs

The M1-mAChR is known to couple to $G_{q/11}$ and activate phospholipase Cβ, leading to PI hydrolysis and intracellular Ca^{2+} mobilization (van Koppen and Kaiser 2003). We examined whether this classical signaling pathway is activated by surface and/or intracellular M1-mAChRs. Carbachol enhanced PI turnover more than twofold in cultured hippocampal neurons (Fig. 3a). This increase was inhibited by the cell-impermeable toxin MT7, as well as by the cell-permeable antagonists pirenzepine and atropine, but not by the M3 antagonist darifenacin. The $G_{q/11}$ inhibitor YM254890 also suppressed the carbachol-stimulated

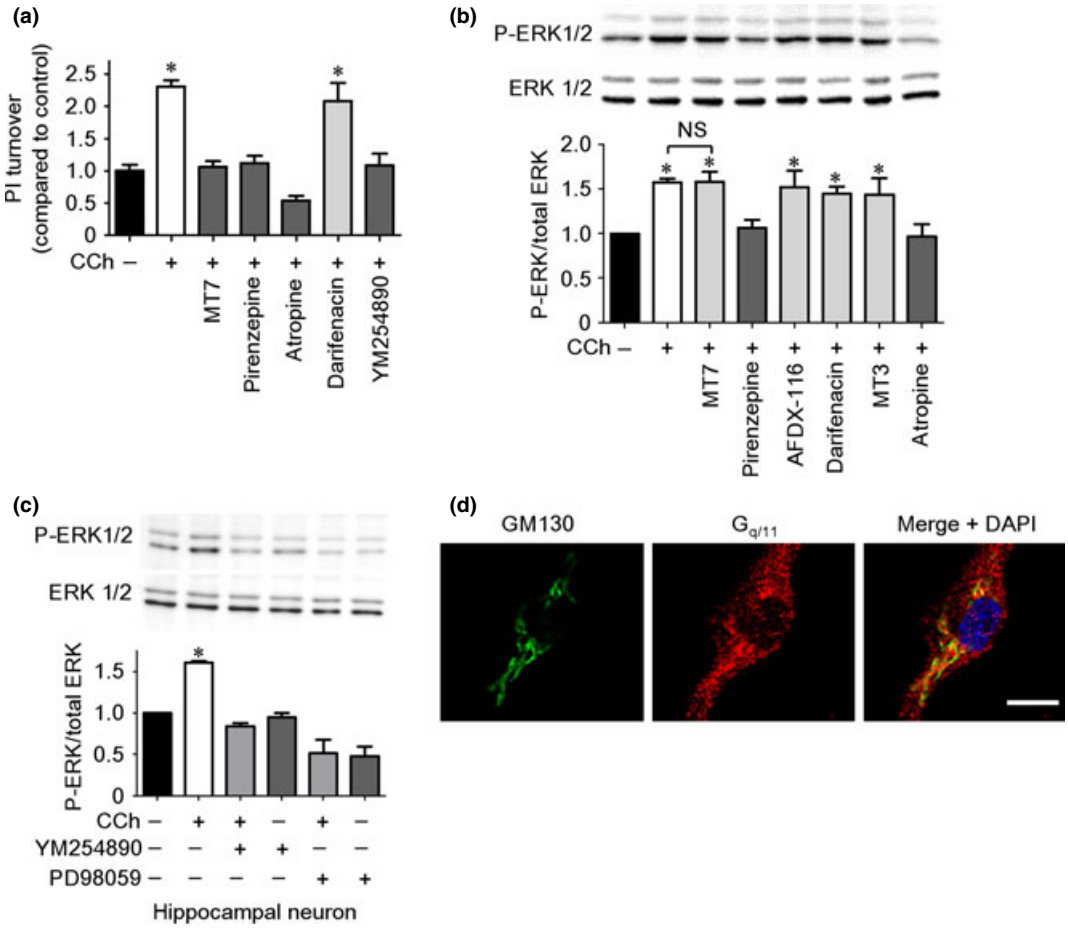

Fig. 3 Distinct signaling activation by surface and intracellular M1-muscarinic acetylcholine receptors (mAChRs) in rat hippocampal neurons. (a) Phosphatidylinositol turnover activated by carbachol (CCh). (b, c) ERK1/2 activation by CCh. The upper panels show representative results. The concentrations used were 100 μM CCh, 0.1 μM MT7, 10 μM pirenzepine, 1 μM atropine, 0.1 μM darifenacin, 0.1 μM MT3, 1 μM AFDX-116, 1 μM YM-254890, 50 μM PD98059. *$p < 0.05$ from basal activity without CCh. NS: not significant. Values represent mean with SEM of three to four experiments. (d) Confocal image of cellular distribution of $G_{q/11}$ protein. Immunostaining of anti-$G_{q/11}$ antibody (red) and anti-GM130 (Golgi marker, green) in hippocampal primary neurons. Merged images include DAPI staining (nucleus, blue). Scale, 10 μm.

increase in PI turnover. The same results were obtained in cortical cultured neurons (data not shown). Thus, the classical signaling pathway is suggested to be selectively activated by surface M1-mAChRs in hippocampal and cortical neurons, which were antagonized by cell-permeable and -impermeable antagonists.

In addition to triggering PI hydrolysis, M1-mAChR has been shown to activate the MAPK/ERK pathway in primary cortical neurons and N1E-115 neuroblastoma cells (Hamilton and Nathanson 2001; Uwada *et al.* 2011). In keeping with these observations, carbachol increased the phosphorylation/activation of ERK1/2 in hippocampal neurons (Fig. 3b). This activation was completely blocked by the cell-permeable antagonists pirenzepine and atropine, but was unaffected by the cell-impermeable M1 antagonist MT7. Other muscarinic antagonists (AFDX-116 for M2 subtype, darifenacin for M3 subtype, and MT3 for M4 subtype) also failed to inhibit carbachol-induced increases in ERK1/2 activation. However, this activation was inhibited by a $G_{q/11}$ inhibitor, YM-254890, and a MAPK/ERK kinase inhibitor, PD98059 (Fig. 3c). $G_{q/11}$-protein is widely distributed at intracellular sites, including Golgi apparatus, in hippocampal neurons (Fig. 3d). From these biochemical analysis together with pharmacological results (Fig. 1b and c), it was strongly suggested that the ERK1/2 pathway was specifically activated through the intracellular M1-mAChRs, and that the activation was selectively antagonized by cell-permeable antagonists but not by cell-impermeable antagonist.

Contribution of surface and intracellular M1-mAChRs to the hippocampal LTP

Activation of M1-mAChRs in the hippocampus is known to facilitate the induction of LTP, linking to cognitive enhancement (Anagnostaras *et al.* 2003). Since intracellular

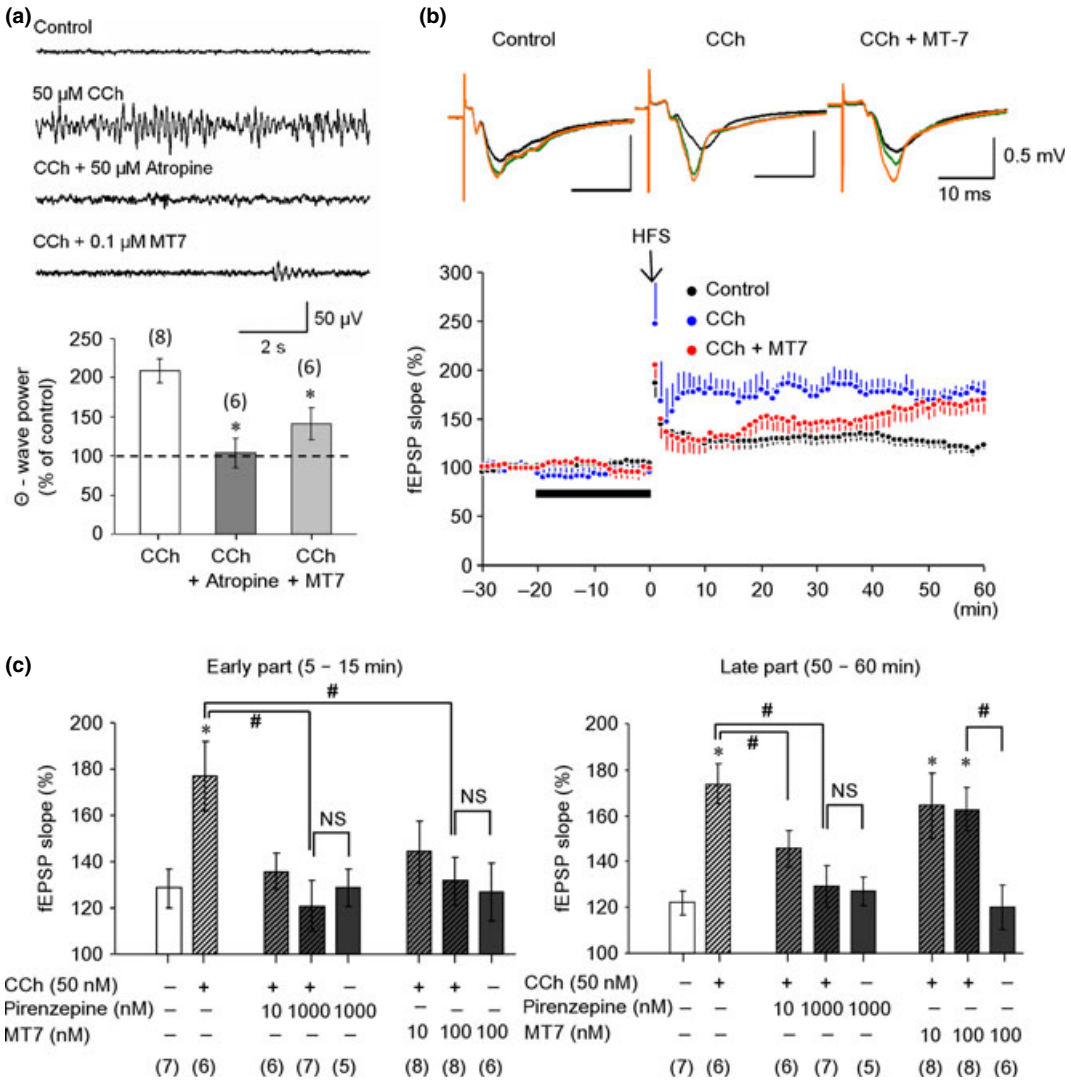

Fig. 4 Theta rhythm induction and long-term potentiation (LTP) facilitation through surface and intracellular M1-muscarinic acetylcholine receptors in rat hippocampal slices. (a) Effects of atropine and MT7 on carbachol (CCh)-induced theta oscillation. $*p < 0.05$ from CCh alone. $*p < 0.05$ from CCh alone. (b) *N*-methyl-D-aspartate receptor-dependent field excitatory post-synaptic potentials (fEPSPs) were recorded on hippocampal pyramidal neurons before and after high-frequency stimulation (HFS) (100 Hz for 1 s, at arrow). Lower panel: time courses of fEPSP slopes in control slices (black circles), and slices pre-treated with CCh (50 nM; blue circles) or with CCh and MT7 (100 nM; red circles) before HFS. Time is expressed relative to HFS application. Horizontal black bar before HFS represents drug application. Upper panel: average traces of fEPSPs at −30 to −20 min (black), 5–15 min (green), and 50–60 min (orange) after HFS are superimposed. (c) Effects of pirenzepine and MT7 on cholinergic facilitation of LTP measured at early (5–15 min) and late (50–60 min) times after HFS. $*p < 0.05$ from control (open column). $^{\#}p < 0.05$ as indicated. NS: not significant. Numbers in parentheses indicate numbers of experiments.

M1-mAChRs were observed in telencephalon, we took an electrophysiological approach to examine how surface and intracellular M1-mAChRs contribute to hippocampal LTP. Hippocampal theta oscillations control the induction of LTP (Huerta and Lisman 1995; Vertes 2005). Carbachol (50 μM, a muscarinic agonist) induced theta rhythm in rat hippocampal CA3 area, which was abolished by atropine and suppressed by cell-impermeable MT7 (Fig. 4a). Carbachol-induced theta oscillations are thus likely to be predominantly mediated by surface M1-mAChRs under the present conditions.

We then focused on NMDAR-dependent LTP in hippocampal CA1 synapses, a classical subject of LTP studies. After HFS (100 Hz, 1 s), LTP was observed as an increase in fEPSP slopes during 60 min (slopes: 128 ± 8% and 122 ± 5% of basal slope at early (5–15 min) and late (50–

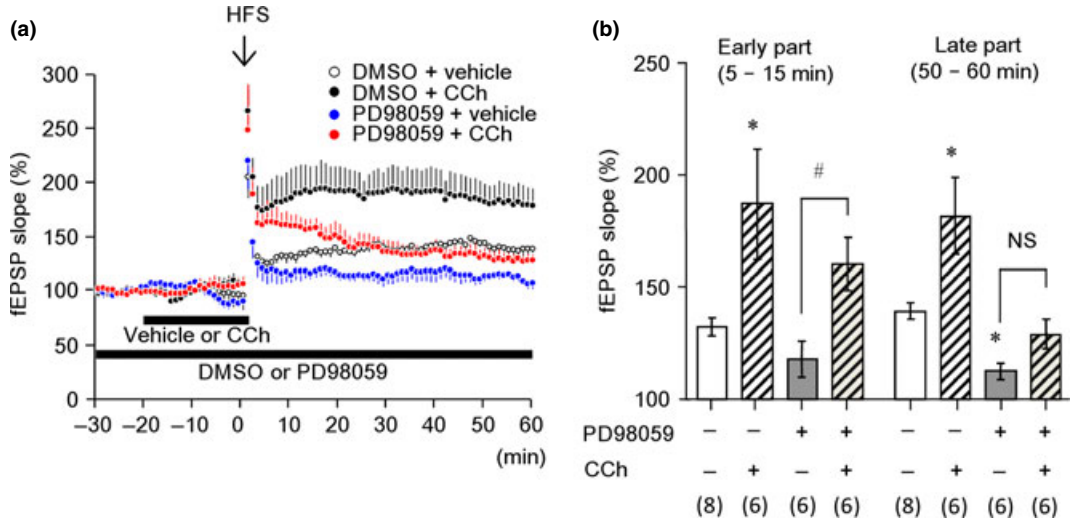

Fig. 5 Involvement of MAPK cascade in carbachol-induced long-term potentiation (LTP) facilitation. (a) Different effects of a MAPK inhibitor (PD98059) on LTP in rat hippocampal slices. Time courses of field excitatory post-synaptic potential slopes in the presence of DMSO or 50 μM PD98059 are shown. Vehicle (open circles) or carbachol (CCh 50 nM, black circles) was pre-treated before high-frequency stimulation (HFS) in the presence of DMSO, while vehicle (blue circles) or carbachol (CCh 50 nM, red circles) in the presence of PD98059. Other conditions are the same as those in Fig. 4b. (b) Effects of 50 μM PD98059 on LTP or its cholinergic facilitation at early (5–15 min) and late (50–60 min) times after HFS. Values represent mean with SEM of six to eight experiments. $^{*}p < 0.05$ from open column (vehicle in the presence of DMSO). $^{\#}p < 0.05$ as indicated. NS: not significant. Numbers in parentheses indicate numbers of experiments.

60 min) times after HFS, respectively) (Fig. 4b and c). Perfusion of 50 nM carbachol before HFS enhanced LTP persistently (177 ± 15% and 174 ± 9% of basal slope at early and late times, respectively). The facilitating effects of carbachol were antagonized by simultaneous treatment with pirenzepine (Fig. 4c), confirming that cholinergic facilitation of LTP depends on M1-mAChRs, as reported previously (Shinoe *et al.* 2005).

Next, we examined the effects of cell-impermeable MT7 on LTP facilitation. Like pirenzepine, simultaneous pre-treatment with MT7 inhibited the early part of carbachol-induced facilitation (132 ± 11% of the basal slope at 5–15 min after HFS at 100 nM MT7), but failed to affect the late part of facilitation (163 ± 9% of basal slope at 50–60 min after HFS at 100 nM MT7) (Fig. 4b and c). Thus, gradual increase in LTP for 20–50 min and its subsequent maintenance were observed in slices pre-treated with both carbachol and MT7. These results suggest that the carbachol-induced facilitation of LTP may be regulated independently through surface and intracellular M1-mAChRs in distinct time-dependent manners. In addition, we tested the effects of the MAPK/ERK kinase inhibitor PD98059 on LTP and its carbachol-induced facilitation. Normal LTP and cholinergically facilitated LTP both were inhibited by 50 μM PD98059, but close inspection revealed that the late stage was more sensitive to MAPK inhibition than the early stage (Fig. 5). The late stage of cholinergic facilitation in LTP may therefore be more dominantly mediated through the ERK1/2 pathway via intracellular M1-mAChR. This result was well consistent to the result reported by English and Sweatt (1997), who showed a more sensitive inhibition by PD98059 at the late phase of HFS-induced LTP than the early phase.

Finally, we examined non-NMDAR-mediated LTP, where a whole-cell patch clamp was applied on CA1 pyramidal neuron at a holding potential of −60 mV in the presence of D-AP5 (an NMDAR antagonist). LTP was induced by application of HFS (100 Hz for 1 s), and the amplitude of EPSCs at 35–40 min after HFS application was compared to that before HFS (Fig. 6a–c). Perfusion of carbachol (50 nM) before HFS enhanced EPSC amplitude to 188 ± 6% of that before HFS, significantly ($p < 0.05$) larger than the control LTP value without carbachol pre-treatment (150 ± 7%, Fig. 6a and d). Combined pre-treatment with MT7 (100 nM) and carbachol (50 nM) did not reduce the enhancement, with EPSC amplitude 198 ± 8% of that before HFS (Fig. 6b and d). On the other hand, simultaneous application of pirenzepine (1 μM) or atropine (1 μM) with carbachol antagonized the carbachol-induced enhancement of LTP (Fig 6c and d). The present electrophysiological analyses thus demonstrated the prominent role of intracellular M1-mAChRs in glutamatergic synaptic plasticity in the CA1 region.

Discussion

This study shows that M1-mAChRs exist not only at the cell surface, but also at intracellular membranes in the hippocampus and other telencephalon regions of rodents

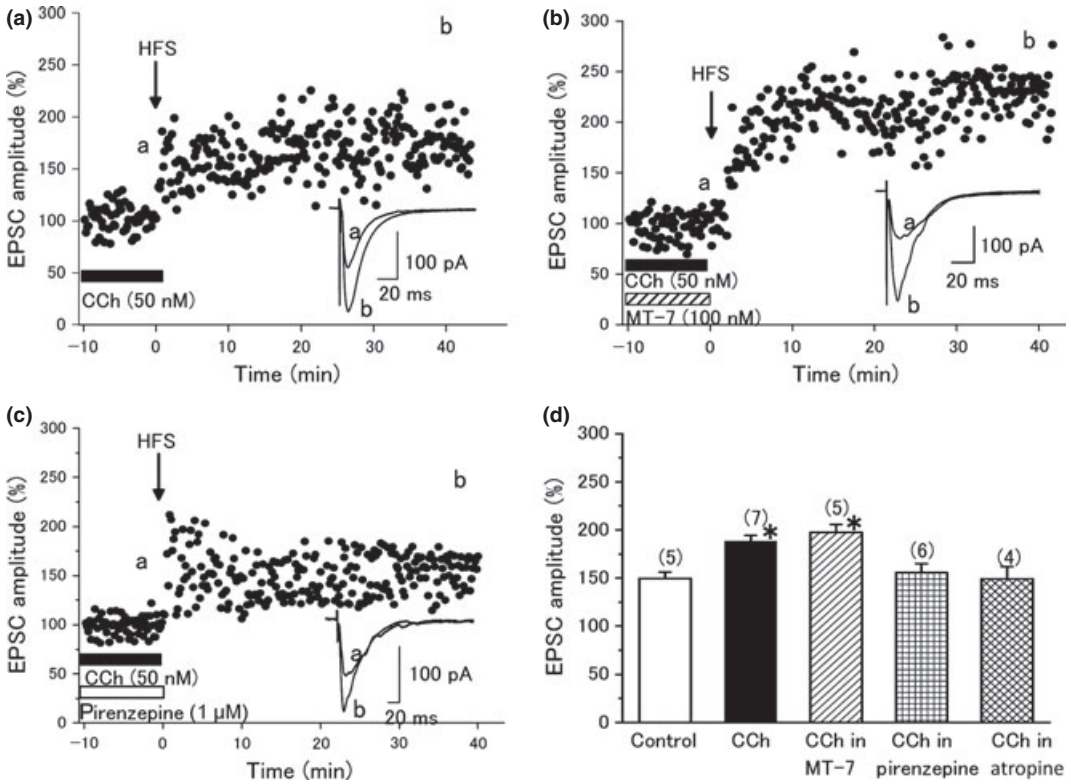

Fig. 6 Modulation of non-*N*-methyl-D-aspartate receptor (NMDAR)-mediated long-term potentiation (LTP) by M1-muscarinic acetylcholine receptors. Whole-cell recordings were made to record non-NMDAR-mediated excitatory post-synaptic currents (EPSCs) in CA1 pyramidal neurons at the holding potential of −60 mV. LTP (increases in the amplitude of EPSCs) was produced by application of high-frequency stimulation (HFS) (100 Hz for 1 s) at arrow. (a–c) Effects of carbachol (CCh, 50 nM) (a), CCh and MT7 (100 nM) (b), and CCh and pirenzepine (1 μM) (c) on EPSCs. Drugs were applied for the period indicated by the horizontal bars before HFS. Inset current traces in each time course plot represent the averages of 10 consecutive responses around the indicated points. (d) Summarized histograms showing the percentage of EPSC amplitude at 35–40 min after HFS compared with that just before HFS. Values represent mean with SEM of five to seven experiments. $*p < 0.05$ from control (open column). Numbers in parentheses indicate numbers of neurons tested. One neuron was examined in each slice, and one or two slices prepared from each animal were used.

and humans, and that M1-mAChRs at both subcellular sites may distinctly contribute to synaptic plasticity in the hippocampus.

Intracellular distribution of functional M1-mAChRs deviates from the classical concept, where intracellular GPCRs including mAChRs represent proteins waiting to enter or having just left the plasma membrane. In this study, however, intracellular distribution was specifically observed only in the M1 subtype among five mAChR subtypes and only in telencephalon. Furthermore, amounts of surface and intracellular M1-mAChRs were comparable under conditions where brain tissues or cultured neurons had not been stimulated. In the brain, M1-mAChRs are known to be selectively expressed in neuronal cells, but not in astroglia (Yamasaki *et al.* 2010). These results suggest that M1-mAChRs constitutively occur at intracellular sites such as Golgi apparatus in telencephalon neurons. Consistent with the present observations, a recent immunoelectron microscopic study demonstrated abundant distribution of M1-mAChRs in the Golgi apparatus and ER of pyramidal neurons (Yamasaki *et al.* 2010). A previous immunohistochemical study with a specific M1-antibody also reported intracellular detection in the cytoplasm of large and small dendrites and dendritic spines of cerebral cortex neurons, although this distribution was taken as evidence of neuronal synthesis of M1-mAChR protein (Mrzljak *et al.* 1993).

Like this study, recent reports have increasingly found that several GPCRs may also be located in and signal from intracellular sites such as ER, Golgi apparatus, and nuclear membranes (Boivin *et al.* 2008; Jong *et al.* 2009; den Boon *et al.* 2012). Interestingly, M1-mAChRs in rat hippocampal and cortical neurons were used in different signaling pathways according to the distinct subcellular location: the PI hydrolysis pathway for surface M1-mAChRs; and the ERK1/2 pathway for intracellular M1-mAChRs. Since

the ERK activation was specifically caused under the conditions where surface mAChR subtypes were masked by MT7 (M1 subtype), AFDX-116 (M2 subtype), darifenacin (M3 subtype), and MT3 (M4 subtype), it is not likely that the present ERK activation is mediated through internalized mAChRs after carbachol binding. Hence, M1-mAChRs at each site may be distinctly activated by carbachol and play distinct physiological functions.

Although the signaling pathways of many intracellular receptors have been studied biochemically, direct involvement in physiological functions has been poorly demonstrated in native tissues. As intracellular M1-mAChRs were specifically detected in the telencephalon, we examined the physiological significance in reference to synaptic plasticity. Cholinergic activation is well known to induce a theta rhythm of neuronal activity and to enhance or induce LTP (Huerta and Lisman 1995; Williams and Kauer 1997; Anagnostaras *et al.* 2003; Shinoe *et al.* 2005; Fernandez de Sevilla *et al.* 2008). Interestingly, our results revealed that the cholinergic induction of theta rhythm and the cholinergic facilitation in early part of NMDAR-dependent LTP were mainly mediated through surface M1-mAChRs, whereas the cholinergic facilitation in the late part of NMDAR-dependent LTP and the majority part of non-NMDAR-dependent LTP was evoked by activation of intracellular M1-mAChRs. Regarding the molecular mechanisms in LTP, many mechanisms have been proposed. The induction of LTP has already been demonstrated to require elevation of post-synaptic calcium (Lynch *et al.* 1983) and activation of protein kinase (Soderling and Derkach 2000), while the maintenance of LTP or its late stage may depend on gene transcription (Nguyen *et al.* 1994; Frey *et al.* 1996), protein synthesis, and post-translational modification (Otani and Abraham 1989; Bliss and Collingridge 1993; Routtenberg and Rekart 2005; Gold 2008). Recent studies have further revealed the involvement of MAPK/ERK cascade in LTP and memory editing (Davis *et al.* 2000; Giovannini 2006). Taking these mechanisms into consideration with the present results, cholinergic facilitation of hippocampal LTP is likely to be regulated by two distinct sites of M1-mAChRs associated with distinct signaling pathways.

Several studies reported that the incidence of synaptic contact between cholinergic varicosities and post-synaptic neurons in the telencephalon was much low [6–14% in rat hippocampus and cerebral cortex (Umbriaco *et al.* 1995; Mechawar *et al.* 2000, 2002); ~3% in mouse hippocampus CA1 region (Yamasaki *et al.* 2010)], although other studies reported relatively higher incidence [66% in rat cerebral cortex (Turrini *et al.* 2001); 67% in the human cerebral cortex (Smiley *et al.* 1997)]. Therefore, two types of cholinergic transmission (phasic synaptic transmission on the scale of seconds and tonic volume/diffuse transmission on the scale of minutes) have been proposed (Descarries *et al.* 1997; Gulledge *et al.* 2009; Yamasaki *et al.* 2010), and the both transmissions may be associated with precisely defined cognitive functions (Parikh *et al.* 2007). The present observations furthermore suggest that not only the synaptic and extrasynaptic surface M1-mAChRs but also the intracellular M1-mAChRs may be involved in cholinergic transmission, regulating synaptic plasticity on multi timescales.

For the intracellular M1-mAChRs to work, cholinergic agonists (ACh or carbachol) must be incorporated into the neurons and cross endosomal membrane. Although information remains lacking about ACh transporters in neuronal tissues, cholinergic agonists have been previously reported to be taken up into mouse cerebral cortex slices (Liang and Quastel 1969). Thus, it is our central issue how ACh is transported, and we are now speculating that intracellular M1-mAChRs in pyramidal neurons of the telencephalon are activated by endogenous and incorporated ACh, although the transporting mechanisms in plasma and endosomal membranes should be elucidated in future studies.

In conclusion, this study demonstrated that M1-mAChRs in telencephalon regions occur not only at the cell surface but also at intracellular sites and may regulate synaptic plasticity. M1-mAChRs have been considered to play important roles in cognitive processes, neuronal cell differentiation, and survival (Everitt and Robbins 1997; Wess 2004; VanDeMark *et al.* 2009), and M1-mAChRs are an important target for the treatment of Alzheimer disease. At present, ACh esterase inhibitors have been clinically used in Alzheimer disease but the detailed mechanisms remain unknown (Pepeu and Giovannini 2010). The present findings would offer novel clues to exploring brain functions such as learning and memory and drug actions in CNS, and furthermore to developing novel drugs for the treatment of neurodegenerative disorders.

Acknowledgements

This study was supported in part by a Grant-in Aid for Scientific Research and the 21st COE Research Program (Medical Science) from the Japan Society of the Promotion of Science (JSPS), a grant from Fukui University, and a grant from the Smoking Research Foundation of Japan. A.S.M.A is supported by the Headquarters for the Advancement of High Priority Research grant, University of Fukui. The authors declare no potential conflict of interests.

References

Anagnostaras S. G., Murphy G. G., Hamilton S. E., Mitchell S. L., Rahnama N. P., Nathanson N. M. and Silva A. J. (2003) Selective cognitive dysfunction in acetylcholine M1 muscarinic receptor mutant mice. *Nat. Neurosci.* **6**, 51–58.

Anisuzzaman A. S. M., Nishimune A., Yoshiki H., Uwada J. and Muramatsu I. (2011) Influence of tissue integrity on pharmacological phenotypes of muscarinic acetylcholine receptors in the rat cerebral cortex. *J. Pharmacol. Exp. Ther.* **339**, 186–193.

Bliss T. V. and Collingridge G. L. (1993) A synaptic model of memory: long-term potentiation in the hippocampus. *Nature* **361**, 31–39.

Boivin B., Vaniotis G., Allen B. G. and Hebert T. E. (2008) G protein-coupled receptors in and on the cell nucleus: a new signaling paradigm? *J. Recept. Signal Transduct. Res.* **28**, 15–28.

den Boon F. S., Chameau P., Schaafsma-Zhao Q. *et al.* (2012) Excitability of prefrontal cortical pyramidal neurons is modulated by activation of intracellular type-2 cannabinoid receptors. *Proc. Natl Acad. Sci. USA* **109**, 3534–3539.

Buzsaki G. (2002) Theta oscillations in the hippocampus. *Neuron* **33**, 325–340.

Caccamo A., Oddo S., Billings L. M., Green K. N., Martinez-Coria H., Fisher A. and LaFerla F. M. (2006) M1 receptors play a central role in modulating AD-like pathology in transgenic mice. *Neuron* **49**, 671–682.

Davis S., Vanhoutte P., Pages C., Caboche J. and Laroche S. (2000) The MAPK/ERK cascade targets both Elk-1 and cAMP response element-binding protein to control long-term potentiation-dependent gene expression in the dentate gyrus in vivo. *J. Neurosci.* **20**, 4563–4572.

Descarries L., Gisiger V. and Steriade M. (1997) Diffuse transmission by acetylcholine in the CNS. *Prog. Neurobiol.* **53**, 603–625.

English J. D. and Sweatt J. D. (1997) A requirement for the mitogen-activated protein kinase cascade in hippocampal long term potentiation. *J. Biol. Chem.* **272**, 19103–19106.

Everitt B. J. and Robbins T. W. (1997) Central cholinergic systems and cognition. *Annu. Rev. Psychol.* **48**, 649–684.

Fellous J. M. and Sejnowski T. J. (2000) Cholinergic induction of oscillations in the hippocampal slice in the slow (0.5-2 Hz), theta (5–12 Hz), and gamma (35–70 Hz) bands. *Hippocampus* **10**, 187–197.

Fernandez de Sevilla D., Nunez A., Borde M., Malinow R. and Buno W. (2008) Cholinergic-mediated IP3-receptor activation induces long-lasting synaptic enhancement in CA1 pyramidal neurons. *J. Neurosci.* **28**, 1469–1478.

Frey U., Frey S., Schollmeier F. and Krug M. (1996) Influence of actinomycin D, a RNA synthesis inhibitor, on long-term potentiation in rat hippocampal neurons in vivo and in vitro. *J. Physiol.* **490**(Pt 3), 703–711.

Giovannini M. G. (2006) The role of the extracellular signal-regulated kinase pathway in memory encoding. *Rev. Neurosci.* **17**, 619–634.

Gold P. E. (2008) Protein synthesis inhibition and memory: formation vs amnesia. *Neurobiol. Learn. Mem.* **89**, 201–211.

Gulledge A. T., Bucci D. J., Zhang S. S., Matsui M. and Yeh H. H. (2009) M1 receptors mediate cholinergic modulation of excitability in neocortical pyramidal neurons. *J. Neurosci.* **29**, 9888–9902.

Hamilton S. E. and Nathanson N. M. (2001) The M1 receptor is required for muscarinic activation of mitogen-activated protein (MAP) kinase in murine cerebral cortical neurons. *J. Biol. Chem.* **276**, 15850–15853.

Huerta P. T. and Lisman J. E. (1995) Bidirectional synaptic plasticity induced by a single burst during cholinergic theta oscillation in CA1 in vitro. *Neuron* **15**, 1053–1063.

Jong Y. J., Kumar V. and O'Malley K. L. (2009) Intracellular metabotropic glutamate receptor 5 (mGluR5) activates signaling cascades distinct from cell surface counterparts. *J. Biol. Chem.* **284**, 35827–35838.

van Koppen C. J. and Kaiser B. (2003) Regulation of muscarinic acetylcholine receptor signaling. *Pharmacol. Ther.* **98**, 197–220.

Langmead C. J., Watson J. and Reavill C. (2008) Muscarinic acetylcholine receptors as CNS drug targets. *Pharmacol. Ther.* **117**, 232–243.

Liang C. C. and Quastel J. H. (1969) Uptake of acetylcholine in rat brain cortex slices. *Biochem. Pharmacol.* **18**, 1169–1185.

Lynch G., Larson J., Kelso S., Barrionuevo G. and Schottler F. (1983) Intracellular injections of EGTA block induction of hippocampal long-term potentiation. *Nature* **305**, 719–721.

Ma L., Seager M. A., Wittmann M. *et al.* (2009) Selective activation of the M1 muscarinic acetylcholine receptor achieved by allosteric potentiation. *Proc. Natl Acad. Sci. USA* **106**, 15950–15955.

Mechawar N., Cozzari C. and Descarries L. (2000) Cholinergic innervation in adult rat cerebral cortex: a quantitative immunocytochemical description. *J. Comp. Neurol.* **428**, 305–318.

Mechawar N., Watkins K. C. and Descarries L. (2002) Ultrastructural features of the acetylcholine innervation in the developing parietal cortex of rat. *J. Comp. Neurol.* **443**, 250–258.

Momiyama T. and Fukazawa Y. (2007) D1-like dopamine receptors selectively block P/Q-type calcium channels to reduce glutamate release onto cholinergic basal forebrain neurones of immature rats. *J. Physiol.* **580**, 103–117.

Mrzljak L., Levey A. I. and Goldman-Rakic P. S. (1993) Association of m1 and m2 muscarinic receptor proteins with asymmetric synapses in the primate cerebral cortex: morphological evidence for cholinergic modulation of excitatory neurotransmission. *Proc. Natl Acad. Sci. USA* **90**, 5194–5198.

Nguyen P. V., Abel T. and Kandel E. R. (1994) Requirement of a critical period of transcription for induction of a late phase of LTP. *Science* **265**, 1104–1107.

Otani S. and Abraham W. C. (1989) Inhibition of protein synthesis in the dentate gyrus, but not the entorhinal cortex, blocks maintenance of long-term potentiation in rats. *Neurosci. Lett.* **106**, 175–180.

Parikh V., Kozak R., Martinez V. and Sarter M. (2007) Prefrontal acetylcholine release controls cue detection on multiple timescales. *Neuron* **56**, 141–154.

Pawlak V., Jensen V., Schupp B. J., Kvello A., Hvalby O., Seeburg P. H. and Kohr G. (2005) Frequency-dependent impairment of hippocampal LTP from NMDA receptors with reduced calcium permeability. *Eur. J. Neurosci.* **22**, 476–484.

Pepeu G. and Giovannini M. G. (2010) Cholinesterase inhibitors and memory. *Chem. Biol. Interact.* **187**, 403–408.

Routtenberg A. and Rekart J. L. (2005) Post-translational protein modification as the substrate for long-lasting memory. *Trends Neurosci.* **28**, 12–19.

Seol G. H., Ziburkus J., Huang S., Song L., Kim I. T., Takamiya K., Huganir R. L., Lee H. K. and Kirkwood A. (2007) Neuromodulators control the polarity of spike-timing-dependent synaptic plasticity. *Neuron* **55**, 919–929.

Shimuta M., Yoshikawa M., Fukaya M., Watanabe M., Takeshima H. and Manabe T. (2001) Postsynaptic modulation of AMPA receptor-mediated synaptic responses and LTP by the type 3 ryanodine receptor. *Mol. Cell. Neurosci.* **17**, 921–930.

Shinoe T., Matsui M., Taketo M. M. and Manabe T. (2005) Modulation of synaptic plasticity by physiological activation of M1 muscarinic acetylcholine receptors in the mouse hippocampus. *J. Neurosci.* **25**, 11194–11200.

Smiley J. F., Morrell F. and Mesulam M. M. (1997) Cholinergic synapses in human cerebral cortex: an ultrastructural study in serial sections. *Exp. Neurol.* **144**, 361–368.

Soderling T. R. and Derkach V. A. (2000) Postsynaptic protein phosphorylation and LTP. *Trends Neurosci.* **23**, 75–80.

Turrini P., Casu M. A., Wong T. P., De Koninck Y., Ribeiro-da-Silva A. and Cuello A. C. (2001) Cholinergic nerve terminals establish classical synapses in the rat cerebral cortex: synaptic pattern and age-related atrophy. *Neuroscience* **105**, 277–285.

Umbriaco D., Garcia S., Beaulieu C. and Descarries L. (1995) Relational features of acetylcholine, noradrenaline, serotonin and GABA axon terminals in the stratum radiatum of adult rat hippocampus (CA1). *Hippocampus* **5**, 605–620.

Uwada J., Anisuzzaman A. S., Nishimune A., Yoshiki H. and Muramatsu I. (2011) Intracellular distribution of functional M(1)

-muscarinic acetylcholine receptors in N1E–115 neuroblastoma cells. *J. Neurochem.* **118**, 958–967.

VanDeMark K. L., Guizzetti M., Giordano G. and Costa L. G. (2009) The activation of M1 muscarinic receptor signaling induces neuronal differentiation in pyramidal hippocampal neurons. *J. Pharmacol. Exp. Ther.* **329**, 532–542.

Vertes R. P. (2005) Hippocampal theta rhythm: a tag for short-term memory. *Hippocampus* **15**, 923–935.

Wess J. (2004) Muscarinic acetylcholine receptor knockout mice: novel phenotypes and clinical implications. *Annu. Rev. Pharmacol. Toxicol.* **44**, 423–450.

Wess J., Eglen R. M. and Gautam D. (2007) Muscarinic acetylcholine receptors: mutant mice provide new insights for drug development. *Nat. Rev. Drug. Discov.* **6**, 721–733.

Williams J. H. and Kauer J. A. (1997) Properties of carbachol-induced oscillatory activity in rat hippocampus. *J. Neurophysiol.* **78**, 2631–2640.

Yamasaki M., Matsui M. and Watanabe M. (2010) Preferential localization of muscarinic M1 receptor on dendritic shaft and spine of cortical pyramidal cells and its anatomical evidence for volume transmission. *J. Neurosci.* **30**, 4408–4418.